(This is a sample cover image for this issue. The actual cover is not yet available at this time.)

Toxicon 135 (2017) 71–83

Contents lists available at ScienceDirect

Toxicon

journal homepage: www.elsevier.com/locate/toxicon

Combined venom profiling and cytotoxicity screening of the Radde's mountain viper (*Montivipera raddei*) and Mount Bulgar Viper (*Montivipera bulgardaghica*) with potent cytotoxicity against human A549 lung carcinoma cells

Ayse Nalbantsoy [a, 1], Benjamin-Florian Hempel [b, 1], Daniel Petras [b, c], Paul Heiss [b], Bayram Göçmen [d], Nasit Iğci [e], Mehmet Zülfü Yildiz [f], Roderich D. Süssmuth [b, *]

[a] Department of Bioengineering, Faculty of Engineering, Ege University, Bornova, 35100, Izmir, Turkey
[b] Technische Universität Berlin, Institut für Chemie, Strasse des 17. Juni 124, 10623, Berlin, Germany
[c] University of California - San Diego, Skaggs School of Pharmacy & Pharmaceutical Sciences, PSB 4231, 9500, Gilman Drive, La Jolla, CA, USA
[d] Zoology Section, Department of Biology, Faculty of Science, Ege University, 35100, Bornova, Izmir, Turkey
[e] Department of Molecular Biology and Genetics, Faculty of Arts and Sciences, Nevşehir Hacı Bektaş Veli University, Nevşehir, Turkey
[f] Zoology Section, Department of Biology, Faculty of Arts and Science, Adıyaman University, Adıyaman, Turkey

ARTICLE INFO

Article history:
Received 12 April 2017
Received in revised form
12 June 2017
Accepted 13 June 2017
Available online 16 June 2017

Keywords:
Montivipera
Mount Bulgar Viper
Radde's mountain viper
Snake venomics
Intact mass profiling
Cytotoxicity

ABSTRACT

Here we report the first characterization of the endemic Mount Bulgar Viper (*Montivipera bulgardaghica*) and Radde's mountain viper (*Montivipera raddei*) venom by a combined approach using intact mass profiling and bottom-up proteomics. The cytotoxicity screening of crude venom as well as isolated serine proteases revealed a high activity against A549 human lung carcinoma cells. By means of intact mass profiling of native and reduced venom we observed basic and acidic phospholipases type A_2. Moreover, the analysis revealed snake venom metalloproteases, cysteine-rich secretory proteins, disintegrins, snake venom serine proteases, C-type lectins, a vascular endothelial growth factor and an L-amino acid oxidase.

1. Introduction

Snake venom is a complex mixture mainly consisting of proteins and peptides (Mackessy, 2010). Although snake venom proteins are grouped into several major protein families, their relative abundance varies depending on the taxonomical category (e.g. inter/intra-specific, inter-genus), as well as geographical region and age (Fry, 2015). Vipers (*Viperidae*, including True Vipers and Pit Vipers) are widespread around the world and are considered as medically important venomous snakes (Fry, 2015; Harvey, 2014). Important major protein families found in Viperid venoms are snake venom metalloproteinase (SVMP), snake venom serine proteinase (SVSP), hyaluronidase, 5'-nucleotidase, phospholipase A_2 (PLA_2), disintegrin, C-type lectin protein (CLP), cysteine-rich secretory protein (CRISP), natriuretic peptide, bradykinin-potentiating peptide (BPP), nerve growth factor (NGF), snake venom vascular endothelial growth factor (VEGF-F), Kunitz-type proteinase inhibitor (İğci and Demiralp, 2012; Mackessy, 2010).

In Turkey, abundant venomous snakes belong to the *Viperinae* subfamily (True Vipers). There is also one Elapid (*Walterinnesia morgani*) with a limited occurrence in Southeastern Anatolia and number of ophistoglyphous snakes in Turkey. Anatolian vipers show a high level of endemism and diversity. In total 14 taxa of vipers (*Viperinae*) have been recorded in Turkey belonging to the genera *Macrovipera*, *Montivipera* and *Vipera*. Mountain Vipers (members of the genus *Montivipera*) consist of a taxonomic species complex and all species in this group are adapted to rocky habitats

* Corresponding author. Technische Universität Berlin, Institut für Chemie, Strasse des 17. Juni 124, 10623, Berlin, Germany.
E-mail address: roderich.suessmuth@tu-berlin.de (R.D. Süssmuth).
[1] Both authors contributed equally to this work.

http://dx.doi.org/10.1016/j.toxicon.2017.06.008
0041-0101/

above 1500 m, except for *Montivipera xanthina* which is also found at sea level (Stümpel et al., 2016). Two species groups are described in this complex based on morphological characters: the *Xanthina* species-group and the *Raddei* species-group (Mallow et al., 2003; Nilson and Andrén, 1986).

Montivipera bulgardaghica (Nilson and Andren, 1986) (Mount Bolkar Viper) is an endemic viper species found in the Bolkar Mountain range (Cilician Taurus) in Southeastern Turkey (Mallow et al., 2003). Its conservation status is listed as "Least Concern" according to IUCN (2015) (IUCN, 2015). The occurrence is limited but in a suitable habitat, which depends on the microstructure, it seems that dense populations not to be under threat. *Montivipera raddei* (Boettger, 1890) (Radde's Mountain Viper) is distributed from Eastern Turkey and Armenia to Azerbaijan and Iran and possibly Iraq with two different subspecies. *M. raddei raddei* subspecies occurs in Turkey (Mallow et al., 2003). It is listed as "Near Threatened" according to IUCN (2015) based on the observable habitat loss within its distribution range (IUCN, 2015).

Besides the medical importance due to envenomation, snake venoms are an attractive source for the discovery of novel bioactive proteins/peptides with potential therapeutic potential. Many snake venom proteins have shown anticancer, antimicrobial, antiplatelet and analgesic properties and a number of them led to the design and development of drugs (Chan et al., 2016; Fox and Serrano, 2007; King, 2015; Lewis and Garcia, 2003; Vetter et al., 2011). A considerable number of proteins with *in vitro* and/or *in vivo* anticancer activity have been identified in snake venoms. These proteins generally belong to the SVMP, PLA_2, LAAO, CLP and disintegrin families (Calderon et al., 2014). *In vitro* studies showed that many crude snake venoms and their purified proteins have a dose-dependent cytotoxic activity against various cancerous and non-cancerous cell lines (Calderon et al., 2014; Jamunaa et al., 2012; Ozen et al., 2015; Suzergoz, 2016; Yalcin et al., 2014). These proteins exert their cytotoxic/anti-proliferative effects through different molecular mechanisms such as necrosis, apoptosis-induction, integrin blocking, alteration of cell cycle proteins and deterioration of the cell membrane integrity (Calderon et al., 2014; Ozen et al., 2015). Researchers have focused on the proapoptotic properties of crude snake venoms and purified venomic proteins (Calderon et al., 2014; Suzergoz, 2016) since many chemotherapeutic agents have been shown to induce apoptosis (Gerl and Vaux, 2005). Elucidation of the molecular mechanisms underlying the cytotoxic activity of active proteins is a further step in order to assess their anti-cancer potential.

Recently, we reported on the venomic and biological characterization of several Turkish vipers (Göçmen et al., 2015; İğci and Demiralp, 2012; Nalbantsoy et al., 2012, 2013; Ozen et al., 2015; Suzergoz, 2016; Yalcin et al., 2014). With regard to the genus *Montivipera*, there is limited information in literature available. In addition these studies are either focused only on the venom characterization (Sanz et al., 2008) or the biological activity of crude venom (Nalbantsoy et al., 2016; Sawan et al., 2017; Yalcin et al., 2014). In the present study, the venom of two Mountain Vipers, *M. bulgardaghica* and *M. raddei* were analyzed by mass spectrometry-based characterization combining classical bottom-up venomics (Calvete et al., 2007; Eichberg et al., 2015; Lomonte and Calvete, 2017; Petras et al., 2011) and intact mass profiling (Petras et al., 2015, 2016). *In vitro* cytotoxic activity of the crude venoms was assessed using various cancer and non-cancerous cells and identified major reversed-phase fractions of the endemic viper *M. bulgardaghica* were further screened for potential anticancer activities. Previous results on the venom characterization of *M. raddei* are limited to the bottom-up approach (Sanz et al., 2008). The mass spectrometry-guided intact profiling in our study expands these results by detecting even small peptides. Further we document the first venom proteome characterization of *M. bulgardaghica* with interesting cytotoxic activities.

2. Material and methods

2.1. Collection and preparation of venom samples

Individuals of *M. bulgardaghica* were collected from Karboğaz forests in Mersin provinces, in altitudes between 1850 and 2000 m (see Graphical Abstract). Crude *M. bulgardaghica* venom was extracted from two male and three female adults, using a paraffin-covered laboratory beaker without exerting pressure on the venom glands. *M. raddei* individuals were collected from Aydınkavak in the Kars province in altitudes between 1400 and 1500 m (see Graphical Abstract). The venom was extracted by the same way from two male and three female adults. For every single species, each extracted venom sample was pooled in one tube and centrifuged at 2000 *g* for 10 min at +4 °C to eliminate cell debris. Supernatants were collected, directly frozen at −80 °C, afterwards lyophilized and finally stored at +4 °C. The study was approved by the Ege University, Local Ethical Committee of Animal Experiment (Number: 2010/43) and a special permission (2011/7110) for field studies was accepted from the Republic of Turkey, Ministry of Forestry and Water Affairs.

2.2. Determination of protein content

Protein concentrations were determined by the Bradford assay (Bradford, 1976) from diluted venom samples (2 mg/mL; ultra-pure water) using a UV/Vis spectrophotometer (Thermo-Scientific, Darmstadt, Germany) at a wavelength of $\lambda = 595$ nm. Bovine serum albumin was used as a reference.

2.3. Cell culture and in vitro cytotoxicity assay

The following cell lines were used for determination of cytotoxicities: HeLa (human cervix adenocarcinoma), A-549 (human alveolar adenocarcinoma), MCF-7 (human breast adenocarcinoma), CaCo-2 (human colon colorectal adenocarcinoma), mPANC96 (human pancreas adenocarcinoma), PC-3 (human prostate adenocarcinoma), U87MG (human glioblastoma astrocytoma) as cancer cells and as non-cancerous cell lines, HEK (human embryonic kidney) and VERO (African green monkey kidney). Cell lines were purchased from ATCC (Manassas, VA, USA). All cells were cultivated in Dulbecco's modified Eagle's medium F12 (DMEM/F12), supplemented with 10% fetal bovine serum (FBS), 2 mM/L glutamine, 100 U/mL of penicillin and 100 mg/mL of streptomycin (Gibco, Visp, Switzerland). The cells were incubated at 37 °C in a humidified atmosphere of 5% CO_2. The cytotoxicity of the crude venoms and fractions were determined using a modified MTT [3-(4,5-dimethyl-2-thiazolyl)-2,5-diphenyl-2H-tetrazoliumbromide)] assay (Mosmann, 1983), which detects the activity of the mitochondrial reductase of viable cells. The assay principle is based on the cleavage of MTT that forms formazan crystals by the cellular succinate-dehydrogenases in viable cells. Insoluble formazan crystals were dissolved by the addition of DMSO to the wells. In order to perform the cytotoxicity assay, all cell lines were cultivated for 24 h in 96-well microtiter plates with an initial concentration of 1×10^5 cells/mL. Afterwards, the cultured cells were treated with different doses of venom or fractions and incubated for 48 h at 37 °C. The plant-derived compound parthenolide was used as a positive cytotoxic control agent. The optical density (OD) was measured in triplicates at 570 nm (with a reference wavelength of 690 nm) by UV/Vis spectrophotometry (Thermo, Bremen, Germany). The percentages of surviving cells in each culture were

determined after incubation with the venom. The viability (%) was determined by the following formula:

%Viable cells: [(absorbance of treated cells)−(absorbance of blank)]/[(absorbance of control)−(absorbance of blank)] × 100

2.4. Determination of half maximal inhibitory concentration (IC_{50})

The IC_{50} values were calculated by fitting the data to a sigmoidal curve and using a four parameter logistic model and presented as an average of three independent measurements. The IC_{50} values were reported at 95% confidence interval and calculations were performed using the Prism 5 software (GraphPad5, San Diego, CA, USA). The values of the blank wells were subtracted from each well of treated and control cells and half maximal inhibition of growth (IC_{50}) were calculated in comparison to untreated controls.

2.5. Morphological studies

The morphological changes of the cells were observed with an inverted microscope (Olympus, Tokyo, Japan) compared to the control group following 48 h treatment.

2.6. Preparation of venom samples for intact profiling

LC-MS profiling was carried out by dissolving crude venom in aqueous 1% (v/v) formic acid (HFo), to a final concentration of 10 mg/mL, and centrifuged at 20,000 *g* for 5 min. Next, 10 μL of dissolved venom was mixed with 10 μL of *tris*(2-carboxyethyl)-phosphine (TCEP, 0.5 M) and 30 μL of citrate buffer (0.1 M, pH 3) to chemically reduce disulfide bonds. The reaction mixture was incubated for 30 min at 65 °C. In the following, the sample was mixed with an equal volume of 1% formic acid and centrifuged at 20,000 *g* for 5 min. Then 10 μL of both, reduced and non-reduced samples, were submitted to HPLC-high-resolution (HR) MS/MS measurements.

2.7. Intact mass profiling

LC-ESI-HR-MS experiments were performed on an LTQ Orbitrap XL mass spectrometer (Thermo, Bremen, Germany) coupled to an Agilent 1260 HPLC system (Agilent, Waldbronn, Germany), using a Suppelco Discovery 300 Å C18 (2 × 150 mm, 3 mm particle size) column. The flow rate was set to 0.3 mL/min and a gradient of 0.1% HFo in water (solution A) and 0.1% HFo in acetonitrile (ACN) (solution B) was used. The gradient started isocratically (5% B) for 5 min, followed by an increase from 5 to 40% B over 85 min, 40–70% over 20 min, followed by a washout at 70% B for 10 min and ended in a re-equilibration phase at 5% B for 10 min. ESI settings were 40 L/min sheath gas; 20 L/min auxiliary gas; spray voltage, 4.8 kV; capillary voltage, 46 V; tube lens voltage, 135 V and capillary temperature, 330 °C. The survey scan was performed with mass resolution (R) of 100,000 (at *m/z* 400). The MS2 spectra were obtained in an information-dependent acquisition (IDA) mode with R = 100,000 (at m/z 400) and two scan events, where the most abundant ion of the survey scan with calculable charge was selected, with 2 micro scans and 500 ms maximal fill time. Scan event 1 contained a CID scan of the most abundant ion with adjusted normalized collision energy to 35%. The default charge state was set to z = 10 and the activation time to 30 msec. The precursor selection window was set to 2 m/z. Dynamic exclusion was performed with a 3 m/z exclusion window for precursor ions with 2 repeats within 10 s. The exclusion list contained maximal 50 ions for a duration of 20 s. The deconvolution of isotopically resolved spectra was carried out by using the XTRACT algorithm of Xcalibur Qual Browser (Thermo, Bremen, Germany). The manually generated de novo sequence tags were searched against the NCBI non-redundant *Viperidae* database (taxid: 8689) (http://blast.ncbi.nlm.nih.gov/Blast.cgi) using the BLASTP algorithm (Altschul et al., 1990).

2.8. Bottom-up venomics

Bottom-up analyses were carried out by dissolving 2 mg of crude venom in aqueous solution, including 1% HFo and 5% acetonitrile (ACN), to a final concentration of 10 mg/mL. Dissolved venom was injected to an Agilent 1260 semi-preparative reverse-phase (RP) HPLC system (Agilent, Waldbronn, Germany) coupled to a Suppelco Discovery Biowide C18 (300 Å pore diameter, 4.6 × 150 mm column size, 3 mm particle size) column. The venom components were eluted with a linear gradient of 0.1% HFo in water (solution A) and 0.1% HFo in ACN (solution B) with a flow rate set to 1 mL/min. The gradient started isocratically (5% B) for 5 min, followed by linear gradients of 5–40% B for 95 min, 40–70% for 20 min, 70% B for 10 min, and finally end with a re-equilibration at 5% B for 10 min. Peak detection was performed by means of UV detection at λ = 214 nm using a diode array detector (DAD). The peak fractions were collected manually, dried overnight in a vacuum centrifuge, were then chemically reduced with dithiothreitol (DTT) and separated via SDS-PAGE (12% polyacrylamide gels) (Laemmli, 1970). Thereafter coomassie-stained bands were excised from the gel and subjected to in-gel digestion. In the first step bands were treated with a reduction solution (10 mM DTT in 25 mM $(NH_4)HCO_3$, pH 8.3, for 30 min at 65 °C), then a alkylation step (50 mM iodoacetamide in 50 mM $(NH_4)HCO_3$, pH 8.3, for 30 min at 25 °C in the dark) is followed, and finally the in-gel trypsin digestion (12 h at 37 °C with 66 ng sequencing-grade trypsin/mL in 25 mM $(NH_4)HCO_3$, 10% ACN; 0.25 mg/sample) was carried out. Samples were dried in a vacuum centrifuge, tryptic peptides were re-dissolved in 20 μL of 5% ACN containing 0.1% HFo and subsequent submitted to LC-MS/MS analysis using a Orbitrap XL hybrid mass spectrometer (Thermo, Bremen, Germany) coupled with an Agilent 1260 HPLC system (Agilent, Waldbronn, Germany), using a flow rate of 0.3 mL/min. The HPLC system is connected with a Grace Vydac 218MSC18 column (2.1 × 15 mm, 5 mm). A gradient was applied using of 0.1% HFo in water (solution A) and in ACN (solution B) and started isocratically with 5% B for 2 min, followed by an increase over 10 min from 5 to 40% B, then 40–99% B over 15 min, 99% B is held for 5 min with a final re-equilibration phase at 5% B for 5 min. MS experiments were performed on an Orbitrap analyzer with R = 15,000 at *m/z* 400 and maximum filling time of 200 ms for both survey and first product ion scans. MS/MS fragmentation of the most intense ion was performed in the LTQ using CID (30 ms activation time); the collision energy was set to 35%. Precursor-ion isolation was performed within a mass window of *m/z* 2. Dynamic exclusion was set up for a mass window of *m/z* 3 for up to 50 precursor ions with a repeat of 2 within 30 s. By means of the DeNovoGUI tool (Muth et al., 2014) annotated MS2 spectra and generated sequence tags were searched against a *Viperidae* (taxid: 8689) non-redundant protein database of UniProtKB/TrEMBL using BLASTP (Altschul et al., 1990).

2.9. Relative toxin quantification

The relative abundances (% of the total venom proteins) of the different protein families were calculated as the ratio of the sum of the areas of the reverse-phase UV214-chromatographic peaks containing proteins from the same family to the total area of venom

protein peaks in the reverse-phase chromatogram according to research group of Calvete (Juarez et al., 2004). If more than one protein was present in a reverse-phase fraction, their proportions were estimated by the relative abundance of deconvoluted high-resolution mass spectra. If co-eluting proteins were observed by SDS-PAGE which was not accessible by mass spectrometry, their relative abundance was estimated by optical signal strength of the Coomassie-stained bands (Calvete, 2014, 2011).

3. Results and discussion

3.1. The venom proteome of Montivipera bulgardaghica and Montivipera raddei

The venomic analysis in this study focusses on the proteomic characterization and the determination of its composition, using the classical bottom-up protocol via RP-HPLC fractionation, SDS-PAGE, tryptic digest and a final de novo sequencing (Bazaa et al., 2005; Calvete, 2011; Calvete et al., 2007; Juarez et al., 2004; Sanz et al., 2006). The classical venomic bottom-up approach which follows a combination of RP-HPLC and subsequent SDS-PAGE separation has the disadvantage that small sized proteins (<5 kDa) and peptides are eventually not retained during the SDS-PAGE separation. To prevent the loss of components during characterization, fractions containing small molecular weight compounds have to be analyzed without SDS-PAGE separation. If only UV absorption is acquired during HPLC fractionation this information might not be given. In this case the intact MS analysis of fractions by either ESI or MALDI is thus necessary which is first time consuming and might not detect small molecules such as tri-peptides due to low m/z cut-off in MALDI or ion suppression in direct infusion nanoESI (Göçmen et al., 2015; Petras et al., 2015). To bypass the limiting factor of the bottom-up approach, we additionally applied an intact venom molecular mass profiling, which has also the advantage to generate an overview of molecular masses from all venom components, including low abundant and low molecular mass compounds, which makes a mass spectrometric analysis of intact venom a preferable approach (Göçmen et al., 2015). The comparison of the native and reduced venom is a further advantage and allows a more specific classification of the proteome by inter- and intramolecular disulfide bonds (Calvete et al., 2007, 2017; Eichberg et al., 2015). These disulfide bridges are an important characteristic for different viper venom protein families (e.g. cysteine-rich proteins, PLA_2). The limited access to the Radde's mountain viper (*Montivipera raddei*) and the low amount of venom was the decisive motivation to perform an intact protein mass profiling from crude venom in order to gather structural information.

3.1.1. Intact mass profiling

An initial intact mass profiling (see Fig. 1A and B) of the venoms of both viper species revealed for the Radde's mountain viper 76 venom components distributed among various mass ranges: 38 (<1 kDa), 20 (1–3 kDa) and 11 (3–7 kDa), which represents ~23% of the venom content (deconvoluted mass spectra are shown in the Supplemental Information). Furthermore, we observed 7 molecular masses in the mass range between 14 and 35 kDa (see Table 1).

The Mount Bulgar viper venom rendered a composition of 76 venom components in total which are distributed as follows: 20 (<1 kDa), 29 (1–3 kDa) and 12 (3–7 kDa), so that the peptide content is ~28% of the complete viper venom. 15 molecular masses

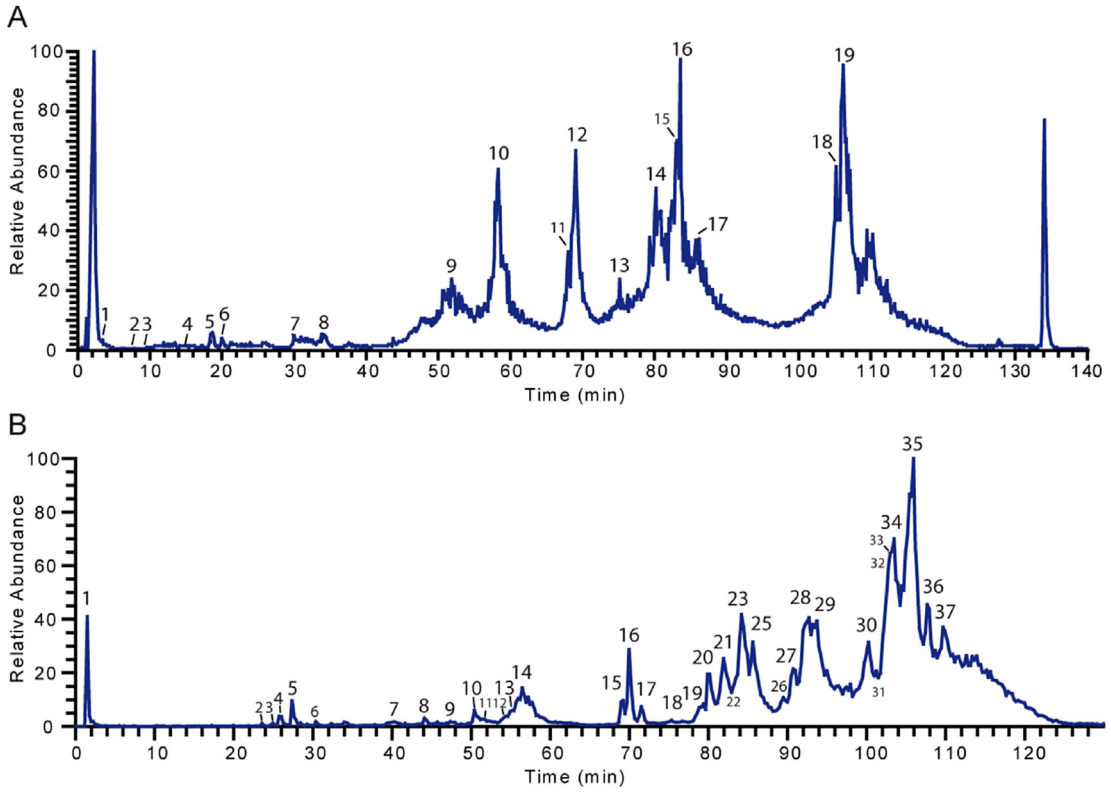

Fig. 1. Intact molecular mass profils of *Montivipera raddei* (A) and *Montivipera bulgardaghica* (B). The UV_{214nm} signal for both chromatograms was set to relative percentage for each highest peak (A: Peak 19 and B: Peak 35) with exception of injection peaks. **A** shows intact mass analysis of the Radde's mountain viper, *Montivipera raddei*. The deconvoluted MS1 spectra of peak 9 and 10 are shown in Fig. 2A and B. Low signal strength of venom compounds due to the of used toxin. **B** shows intact mass analysis of the Mount Bulgar Viper Venom, *Montivipera bulgardaghica*. The deconvoluted MS1 spectra of peak 14b and deconvoluted MS2 spectra of peak 14a are shown in Fig. 2C and D. [Molecular masses, sequence tags and database hits are listed in Tables 1 and 2].

were detected in the mass range between 12 and 55 kDa (see Table 2).

In addition to the measurements of the native venom, the same venom was investigated subsequent to chemical reduction using TCEP. The comparison of native and reduced components and the accompanying exact mass shifts facilitated the determination of the number of disulfide linkages and thus represents a useful tool for the preliminary classification of toxins into putative protein families. The mass profiling for the Radde's mountain viper showed for Peaks 9 and 10 two compounds with a mass shift of +14 Da between native and reduced venom (see Fig. 2A and B). The increase of the molecular mass matches to 7 intramolecular disulfide linkages. The presence of 7 disulfide linkages is a well-described characteristic and specific for the PLA_2 protein family, which is one of the major components of viper venoms (Calvete et al., 2007; Kini, 1997). Furthermore, we also directly identified Peak 14 from

Table 1
Venom peptides and proteins identified from Montivipera raddei. Protein assignment of RP-HPLC fractions (Fig. 3A) by LCMS and MS/MS analysis. Peak numbering corresponds to the UV and MS chromatograms. Sequence tags are obtained by de novo analysis of intact protein and tryptic peptide MS/MS spectra. Protein IDs are obtained by BLASTP analysis of the sequence tags against a viperid non-redundant protein database (taxid: 8689). Molecular weights were determined by SDS-PAGE and intact mass profile analysis and are shown as average masses.

Peak Number	Method	M_{av} [Da]	Identification sequence tag	Protein ID	BLAST E-value	NCBI accession number	RT	Intact mass *m/z* native	*z*	Intact mass RT
1	intact mass MS1	–	–	unknown (~peptide)	–	–	4.174	440.29, 570.33, 636.35, 658.34, 782.44, 765.40, 979.36, 924.31, 1437.43, 5134.74	–	4.20
2	intact mass MS1	–	–	unknown (~peptide)	–	–	5.751	440.28, 657.23, 803.29, 917.41, 943.52, 1202.28, 2403.95, 3217.32	–	7.64
3	intact mass MS1	–	–	unknown (~peptide)	–	–	8.541	440.29, 657.23, 803.29, 933.45, 1095.51, 1298.58, 1532.60, 1897.79, 2403.97	–	9.06
4	intact mass MS1	–	–	unknown (~peptide)	–	–	16.307	460.22, 572.28, 629.25, 645.23, 777.45, 955.30, 1066.48, 3622.40	–	15.57
5	intact mass MS1	–	–	unknown (~peptide)	–	–	22.353	444.22, 476.2, 805.45, 887.44, 1330.65, 3549.74, 3992.96, 4436.18	–	18.70
6	intact mass MS1	–	–	unknown (~peptide)	–	–	23.677	407.21, 805.45, 1072.58, 1230.46, 1964.87, 4024.89	–	20.12
7	intact mass MS1	–	–	unknown (~peptide)	–	–	34.087	648.41, 865.34, 924.52, 1072.59, 3449.06, 7280.35, 7325.40, 7440.42,	–	31.62
8	intact mass MS1	–	–	unknown (~peptide)	–	–	36.787	733.29, 737.29, 765.28, 907.50, 1148.57,1443.59	–	34.43
9	de novo from trypsin digest, intact mass MS1	14	SYNFQDGNLVCGNK FVHDCCYGK	Phospholipase A2 (svPLA2)	3.00E-07 5.00E-05	P31854.2 AHJ09559.1	53.908	1542.10	9	51.37
10a	de novo from trypsin digest	17.5	DLTACVCVLSR	Venom nerve growth factor (VEGF-F)	1.90E-02	P25428.2	60.810	–	–	58.18
10b	de novo from trypsin digest, intact mass MS1	14	FFVHDCCYGR NGDLVCGGNDQLER	Phospholipase A2 (svPLA2) ammodytin I1(A) variant	2.00E-05 6.00E-03	CAE47140.1 JAS04488.1	60.810	1521.11	9	58.18
11	de novo from trypsin digest, intact mass MS1	24	–	unknown (~protein)	–	–	68.431	1300.40	19	68.01
12	de novo from trypsin digest, intact mass MS1	24	FYVCQYCPAGNL	Cysteine-rich venom protein (CRVP)	2.00E-07	XP_015678374.1	68.952	1552.03	16	69.04
13	–	–	–	unknown (~peptide)	–	–	75.374	376.26, 421.32, 2134.55, 2567.35, 2635.84, 2770.22	–	76.72
14	de novo from trypsin digest	35	VVCAGLWQNK	Snake venom serine protease (SVSP)	2.60E-02	E5AJX2.1	79.789	2516.89	14	79.33
15	de novo from trypsin digest	35	VVCAGLWQGGK LMGWGTLSTTK	Snake venom serine protease (SVSP)	1.00E-04 8.00E-04	E5AJX2.1 ADI47567.1	80.555	2585.89	15	80.18
16	de novo from trypsin digest	35	VVCAGLWQGGK MLGWGTLSTTK	Snake venom serine protease (SVSP)	1.00E-04 2.70E-02	E5AJX2.1 ADI47567.1	81.399	2461.91	12	83.55
17	–	60	YNSDLTVLR	Metalloproteinase	2.90E-01	ADI47687.1	83.191	–	–	83.55
18a	–	60	SVGLLQDYCK FSVGVLQDYCK	Metalloproteinase	1.00E-03 1.00E-03	AHB62069.1 ADI47642.1	104.412	–	–	104.72
18b	de novo from trypsin digest	30	–	unknown (~protein)		–	104.412	–	–	104.72
19a	de novo from trypsin digest	60	–	unknown (~protein)		–	106.991	–	–	106.16
19b	de novo from trypsin digest	30	–	unknown (~protein)		–				

Table 2
Venom peptides and proteins identified from *Montivipera bulgardaghica*. Protein assignment of RP-HPLC fractions (Fig. 3B) by LCMS and MS/MS analysis. Peak numbering corresponds to the UV and MS chromatograms. Sequence tags are obtained by de novo analysis of intact protein and tryptic peptide MS/MS spectra. Protein IDs are obtained by BLASTP analysis of the sequence tags against a viperid non-redundant protein database (taxid: 8689). Molecular weights were determined by SDS-PAGE and intact mass profile analysis and are shown as average masses.

Peak Number	Method	M_{av} [Da]†, ‡	Identification sequence tag	Protein ID	BLAST E-value	NCBI accession number	RT	Intact mass *m/z* native	*z*	Intact mass RT
1	intact mass MS1	–	–	unknown (~peptide)	–	–	2.189	429.04; 643.03; 835.06; 1071.05	–	1.47
2	intact mass MS1	–	–	unknown (~peptide)	–	–	22.582	435.33; 785.15; 1023.60; 1731.87; 1801.72; 2107.09; 2666.15; 4040.88	–	22.92
3	intact mass MS1	–	–	unknown (~peptide)	–	–	23.604	443.22; 886.43; 922.41; 1784.70; 2031.79; 3164.45; 4039.87; 4651.88	–	23.56
4	intact mass MS1	12	LQGLVSWGSGCAQK	Thrombin-like enzyme gyroxin (SVTLE)	4.00E-03	Q58G94.1	24.131	1062.63	5	24.39
5	intact mass MS1	–	–	unknown (~peptide)	–	–	25.297	429.16; 858.33; 1071.58; 1287.49; 1500.74; 3156.32	–	25.77
6	intact mass MS1	–	–	unknown (~peptide)	–	–	27.971	671.30; 795.77; 1005.72; 1071.57; 3608.68; 4023.86	–	27.38
7	intact mass MS1	–	–	unknown (~peptide)	–	–	39.307	721.42; 920.46; 1018.52; 1132.58; 2667.02; 6951.84	–	40.02
8	intact mass MS1	12	GLNDYCTKSSDCPR	Disintegrin EMS11A	1.00E-06	P0C6A3.1	42.063	1442.22	10	44.12
9	de novo from trypsin digest, Intact mass MS1	–	–	unknown (~peptide)	–	–	43.606	721.42; 920.46; 1018.52; 1132.57; 1577.78; 6390.66	–	47.40
10a	de novo from trypsin digest, intact mass MS1	14	HTVDMQLMR PFPDVFQR	Snake venom vascular endothelial growth factor (VEGF-F)	8.00E-04 2.10E-02	P82475.2	48.209	1422.80	10	49.59
10b	de novo from trypsin digest	12	KDDYCTGLSSDCPR	Disintegrin VLO5A	6.00E-08	P0C6A9.1	48.209	1538.44	9	
11a	de novo from trypsin digest, intact mass MS1	14	HTVDMQLMR PFPDVFQR	Snake venom vascular endothelial growth factor (VEGF-F)	8.00E-04 2.10E-02	P82475.2	49.340	1447.42	10	50.42
11b	de novo from trypsin digest	12	KDDYCTGLSSDCPR	Disintegrin VLO5A	6.00E-08	P0C6A9.1	49.340	1435.37	9	
12	intact mass MS1	–	–	unknown (~peptide)	–	–	51.264	622.33; 1002.50; 1115.58; 1327.70; 1350.70 1383.63;	–	51.19
13	intact mass MS1	–	–	unknown (~peptide)	–	–	53.141	622.33; 1002.50; 1115.58; 1327.70; 1350.70 1383.63;	–	51.45
14a	de novo from trypsin digest, intact mass MS1	15	NGDLVCGDGDPCLR YSFENGDLVCGG NLYQFQGMLFKMTR	acidic phospholipase A2 (svPLA2)	4.00E-07 3.00E-06 1.00E-05	F8QN51.1	56.692	–	–	56.45
14b	de novo from trypsin digest, intact mass MS1	14	SYNFQNGNLVCGNK SFEDGDLVCGGD	basic phospholipase A2 (svPLA2)	1.00E-08 4.00E-05	P31854.2	56.692	1367.5	10	56.45
15a	de novo from trypsin digest	15	NGDLVCGDGDPCLR YSFENGDLVCGG NLYQFQGMLFKMTR	acidic phospholipase A2 (svPLA2)	4.00E-07 3.00E-06 1.00E-05	F8QN51.1	66.066	–	–	67.56
15b	de novo from trypsin digest, intact mass MS1	14	YSFENGDLVCGG NGDLVCGGDDNQKR	neutral phospholipase A2 (svPLA2)	3.00E-06 6.00E-04	P34180.2	66.066	1520.55	9	67.56
16a	de novo from trypsin digest	40	LYDAYPEAAANAER	prepro-cysteine-rich venom protein (CRVP)	7.00E-05	AAB48565.1	66.902	–	–	69.96
16b	de novo from trypsin digest, intact mass MS1	25	MEWYPEAAANAER KPELQYLLDLHNTLR	Cysteine-rich venom protein (CRVP)	7.00E-05 5.00E-03	AAB48565.1	66.902	1379.7	18	69.96
17	intact mass MS1	–	–	unknown (~peptide)	–	–	68.759	436.34; 478.30; 1724.01; 4428.24; 4483.32; 5312.7	–	74.50
18	de novo from trypsin digest	44‡	LQGLVSWGSGCAQK	Venom serine proteinase-like HS120 (SVSP)	3.00E-03	Q5W958.1	70.801	–	–	75.06
19	de novo from trypsin digest	45	TLCAGLLEGGLDSCK LMGWGTLTTTK	serine protease, rhinocerase 3 (SVSP)	3.00E-07 2.00E-04	CBM40646.1	72.875	–	–	75.33
20a	de novo from trypsin digest	40	GTLLNQEWVLTAAR	serine protease (SVSP)	4.00E-08	BAN82028.1	74.1	–	–	76.97
20b	de novo from trypsin digest, intact mass MS1	32	LTLNQEWVLTAAR LSLLNQEWVLTKK	Thrombin-like enzyme (SVTLE)	3.00E-06 7.00E-05	P0DL27.1	74.1	2253.48	15	76.97
21	de novo from trypsin digest, intact mass MS1	35	GTLLNQEWVLTAAR LTLNQEWVLTAAR	serine protease (SVSP)	4.00E-08 3.00E-06	BAN82028.1	75.855	1395.95	21	80.15
22		60	LVLVVDHSMVEK		2.00E-05	ADI47715.1	77.161	–	–	–

Table 2 (*continued*)

Peak Number	Method	M_{av} [Da]†, ‡	Identification sequence tag	Protein ID	BLAST E-value	NCBI accession number	RT	Intact mass *m/z* native	*z*	Intact mass RT
	de novo from trypsin digest, intact mass MS1		YYLVNEMYLPLNLR	Zinc metalloproteinase (SVMP)	9.00E-06					
23a	de novo from trypsin digest	60	ANTVNEFYLPLNLR VTSSGDDTLDSFEK	metalloproteinase (SVMP)	5.00E-06 3.00E-05	ADI47591.1	78.830	1509.88	20	85.65
23b	de novo from trypsin digest, intact mass MS1	35	LMGWGTLSTTK	serine protease (SVSP)	8.00E-04	ADI47567.1	78.830	–	–	85.65
23c	de novo from trypsin digest, intact mass MS1	13	LQGLVSWGSGCAQK	Thrombin-like enzyme gyroxin (SVTLE)	4.00E-03	Q58G94.1	78.830	886.24	16	85.65
24	de novo from trypsin digest	55	–	unknown (~protein)	–	–	81.532	–	–	86.14
25a	de novo from trypsin digest	55	VNLLNEMYLPLNLR	metalloproteinase (SVMP)	5.00E-06	ADI47590.1	82.815	1509.73	20	86.89
25b	de novo from trypsin digest, intact mass MS1	12	AWSDEPNCFVAK LQGLVSWGSGCAQK EEAEQFCTESLR	C-type lectin-like protein, Snaclec subunit β (CTL)	4.00E-08 2.00E-04 1.00E-03	B4XT06.1	82.815	890.36	15	86.89
26	de novo from trypsin digest	60	VQCESGECCEQCR AVATSEQQSYYDR SELVSPPVCGQEVLEK VSSSDNTLNSFW	Zinc metalloproteinase, Adamalysin II (SVMP)	2.00E-09 2.00E-07 3.00E-05 4.00E-03	U5PZ28.1	86.152	–	–	90.72
27	de novo from trypsin digest	50	VQCESGECCEQCR	Zinc metalloproteinase (SVMP)	2.00E-09	U5PZ28.1	87.103	–	–	91.72
28	de novo from trypsin digest	50	AVQCESGECCEQCR	Zinc metalloproteinase (SVMP)	2.00E-09	U5PZ28.1	88.306	–	–	92.71
29	de novo from trypsin digest	48	–	unknown (~protein)	–	–	90.071	–	–	94.94
30	de novo from trypsin digest	45	LQGLVSWGSGCAQK	serine protease, trypsinogen homolog (SVSP)	2.00E-04	AAF01343.1	98.185	–	–	100.22
31	de novo from trypsin digest	45	FNLSCGDDYPFVCK	C-type lectin-like protein, Snaclec subunit β (CTL)	2.00E-10	W5XCJ6.1	100.558	–	–	102.47
			SKNEGTNCFVFK	C-type lectin-like protein 3B (CTL)	1.00E-05	AJO70723.1				
32	de novo from trypsin digest	65	LYEFVNTLNVVMR	metalloproteinase H4-A (SVMP)	2.00E-04	AHB62069.1	101.481	–	–	103.46
33	de novo from trypsin digest	55	–	unknown (~protein)	–	–	102.164	–	–	104.45
34	de novo from trypsin digest	65	–	unknown (~protein)	–	–	103.857	–	–	105.44
35	de novo from trypsin digest	65	–	unknown (~protein)	–	–	104.742	–	–	105.93
36	de novo from trypsin digest	60	VNLLNEMYLPLNLR VPLVGVELWDNR	metalloproteinase (SVMP)	5.00E-06 4.00E-03	ADI47590.1	106.659	–	–	107.66
37	de novo from trypsin digest	50	NVEEGWYANLGPMR	L-amino acid oxidase (LAAO)	1.00E-08	G8XQX1.1	107.691	–	–	109.65
			SCLMSGTLSCEASLR	H3 metalloproteinase precursor 1 (SVMP)	1.00E-07	AGL45259.1				

the Mount Bulgar viper as a PLA_2 species through the observed mass shift of +14 Da in the reduced sample compared to the native sample (see Fig. 2C). The manual annotation of a subsequent MS2 spectrum from the chemically reduced Mount Bulgar venom and the search of generated sequences against a *Viperidae* database (Blast algorithm, taxid: 8689) helped to identify the sequence tag (2043)-NJSYSDYGCCG-(1986) for a further PLA_2 (see Fig. 2D). The molecular mass of the deconvoluted MS1 spectra (5490.50 Da) is much lower than the expected size for proteins of the PLA_2 (12–14 kDa) family, which are described in literature (Six and Dennis, 2000) and would correspond to the band height of the SDS-PAGE analysis of the isolated Peak 14a. We speculate that the fragmentation of PLA_2 may have occurred during the sample preparation with TCEP.

3.1.2. Bottom-up venomics

In addition to our initial intact molecular mass profiling, we also investigated the venoms via a bottom-up approach, i.e. by HPLC fractionation, SDS-PAGE separation (see Fig. 3a and b) followed by in-gel digestion and LC-MS/MS analysis. The venom content for both species is illustrated in a pie chart (see Fig. 4) and contains the major *Viperidae* toxin families. Apart from peptides, the most abundant toxin family of the Radde's mountain viper is represented by snake venom phospholipases A_2 (svPLA$_2$, 26.02%) followed by serine proteases (svSP, 14.09%), metalloproteases (svMP, 11.54%), vascular endothelial growth factors (VEGF-F, 8.33%), cysteine-rich secretory proteins (CRISP, 4.15%) and some non-characterized proteins (7.70%). In contrast the most abundant toxin families from the Mount Bulgar viper is represented by snake venom metalloproteases (svMP, 15.95%) followed by phospholipases A_2 (svPLA$_2$, 15.19%), serine proteases with associated thrombin-like enzymes (svSP, 10.90%), cysteine-rich secretory proteins (CRISP, 4.46%), as well as C-type lectins (CTL, 3.91%), disintegrins (2.12%), L-amino acid oxidases (LAAO, 1.42%), vascular endothelial growth factors (VEGF-F, 0.75%) and some proteins (22.76%) which could not be assigned to a dedicated function. The high proportions of non-annotated proteins can be explained by the usage of MS/MS de novo sequence tags for databases identification. As no genome or transcriptome data is available for *Montivipera raddei* and *Montivipera bulgardaghica* the identification relied mainly on toxin

homologs from other viper species in the NCBI database. Besides the general lower accuracy rate of de novo protein assignment in comparison to peptide spectrum matching (PSM), the missing low mass m/z range in collision-induced fragmentation in the linear ion trap of the mass spectrometer typically results in the absence of b1 and y1 ions. This often impede the generation of de novo sequence tags with significant database hits. The quantification of various toxin families in the bottom-up approach relies on the detectable UV signal from the HPLC run, which in turn depends on the concentration and the respective molar extinction coefficient ε in a defined absorbing wavelength ($\lambda = 214$ nm). Therefore, the absence of some typical venom components in the Radde's mountain venom (e.g. disintegrins, C-type lectin or L-amino acid oxidase) can be explained by the bottom-up workflow. Genomic or transcriptomic analysis of the venom gland tissues, which however could not be performed within this study, would significantly help to improve the accuracy of the spectra annotation. The incomplete venom characterization of the Radde's mountain viper makes it difficult to compare the venom composition of both species while previous bottom-up studies report on the toxin families disintegrins, C-type lectin and L-amino acid oxidase (Sanz et al., 2008).

The comparison of the venom composition of the Mount Bulgar viper with those reported of the Radde's mountain viper (Sanz et al., 2008) shows a similar content for snake venom metalloproteases (both 9 proteins), CRISP's (both 2 proteins) and LAAO (both 1 protein). The content of C-type lectin (2 proteins vs. 3 proteins) and VEGF-F (2 proteins vs. 1 protein) show small differences. In contrast, phospholipase A_2 (4 proteins vs. 2 proteins), disintegrins (3 proteins vs. 5 proteins) and especially serine proteases (7 proteins vs. 4 proteins) differ strongly between the two *Montivipera* populations. In addition, Kunitz-type inhibitor and DC-fragment are absent in the Mount Bulgar viper venom.

3.2. Cytotoxicity screening

Snakes and their venomous cocktails potentially contain new compounds of therapeutic interest (Shanbhag, 2015). The first phase of anticancer drug discovery related to venom research aims to determine the cytotoxic potential with an initial screening study as part of a bioactivity-guided characterization process (Fox and Serrano, 2007; Göçmen et al., 2015; Harvey, 2014; Yalcin et al., 2014). The *Montivipera* genus, part of the *Viperidae* family, is a rarely studied species. Previously published results showing the *in vitro* cytotoxic activity of different *Montivipera* species, like *Montivipera xanthina* (Ottoman Viper) (Yalcin et al., 2014), endemic *Montivpera wagneri* (Wagner's Viper) (Nalbantsoy et al., 2016) or recently published *Montivipera bornmuelleri* (Sawan et al., 2017), which was tested on various cancer cell lines. In the present study, cytotoxicity assays of the *Montivipera bulgardaghica* and *Montivipera raddei* crude venoms were performed for different cancer (CaCo-2, MCF-7, U87MG, HeLa, MPanc-96, A549, PC3) and non-cancerous (HEK293, Vero) cell lines. Both venoms showed concentration-dependent cytotoxic activity at various levels (see Fig. 5). The calculated IC_{50} values for each cell lines following 48 h venom treatment varied between 2.60 and 9.22 μg/mL for *M. bulgardaghica* and 0.65–46.84 μg/mL for *M. raddei* (see Table 3).

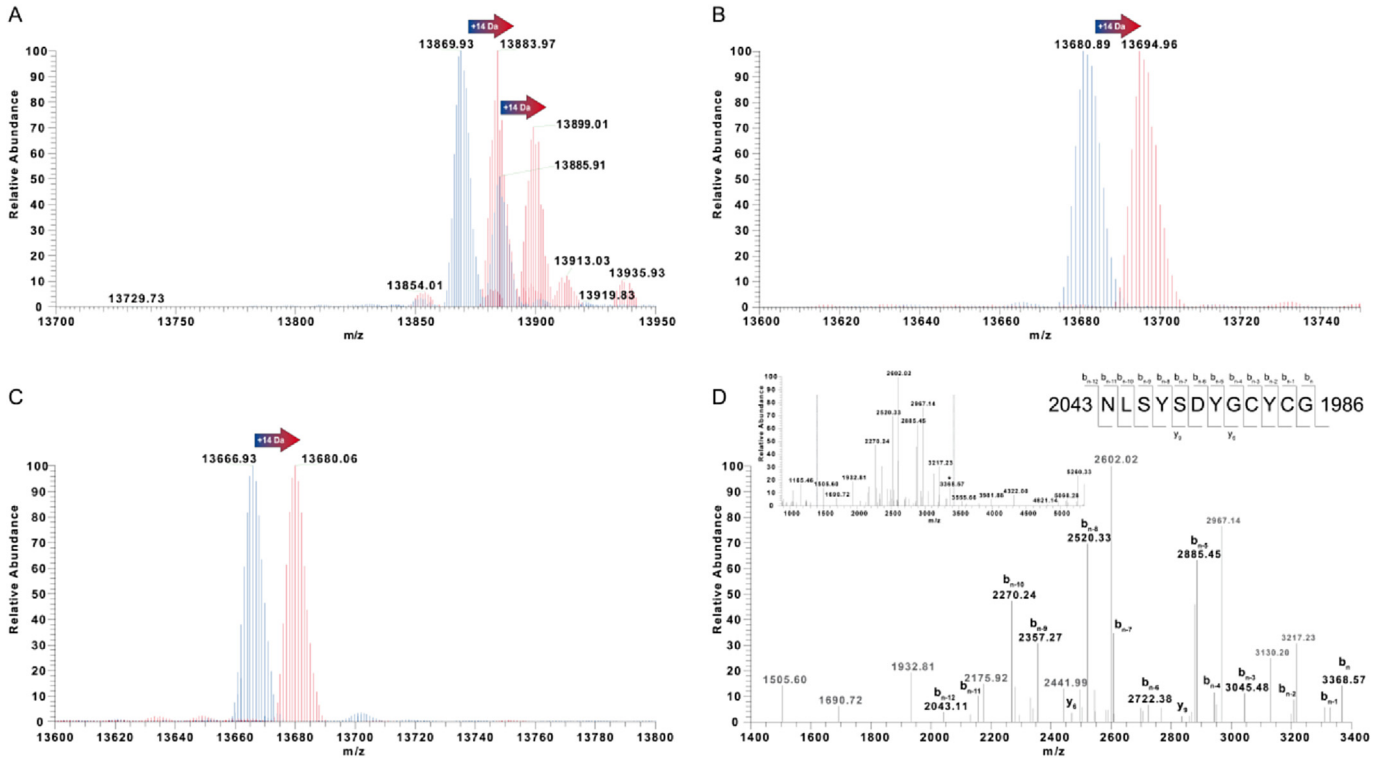

Fig. 2. Denconvoluted MS1 spectra of native and chemically reduced *Montivipera* venoms. A The deconvoluted MS1 spectrum of peak 9 from *M. raddei* with molecular masses of 13869.9 Da and 13885.9 Da (average masses) for native venom (blue) and molecular masses of 13883.9 Da and 13899.0 (average masses) for reduced venom (red). The comparison of native and reduced intact venom species shows a mass shift of Δ14 Da, which is attributed to seven reduced disulfide bridges and is a typical characteristic of phospholipases A_2. **B** The deconvoluted MS1 spectrum of peak 10 from *M. raddei* with molecular mass of 13680.9 Da (average mass) for native venom (blue) and molecular mass of 13694.9 Da (average mass) for reduced venom (red). Again the mass shift of native and reduced intact venom species is Δ14 Da, which is attributed to seven reduced disulfide bridges a typical characteristic of phospholipases A_2. **C** The deconvoluted MS1 spectrum of peak 14b from *M. bulgardahica* with molecular mass of 13666.9 Da (average mass) for native venom (blue) and molecular mass of 13680.9 Da (average mass) for reduced venom (red). **D** The deconvoluted MS2 spectra of the 6 times charged precursor (916.09 m/z) for peak 14a from *M. bulgardahica* is shown. The y-ions and b-ion series is annotated, the resulting sequence tag is displayed above. (For interpretation of the references to colour in this figure legend, the reader is referred to the web version of this article.)

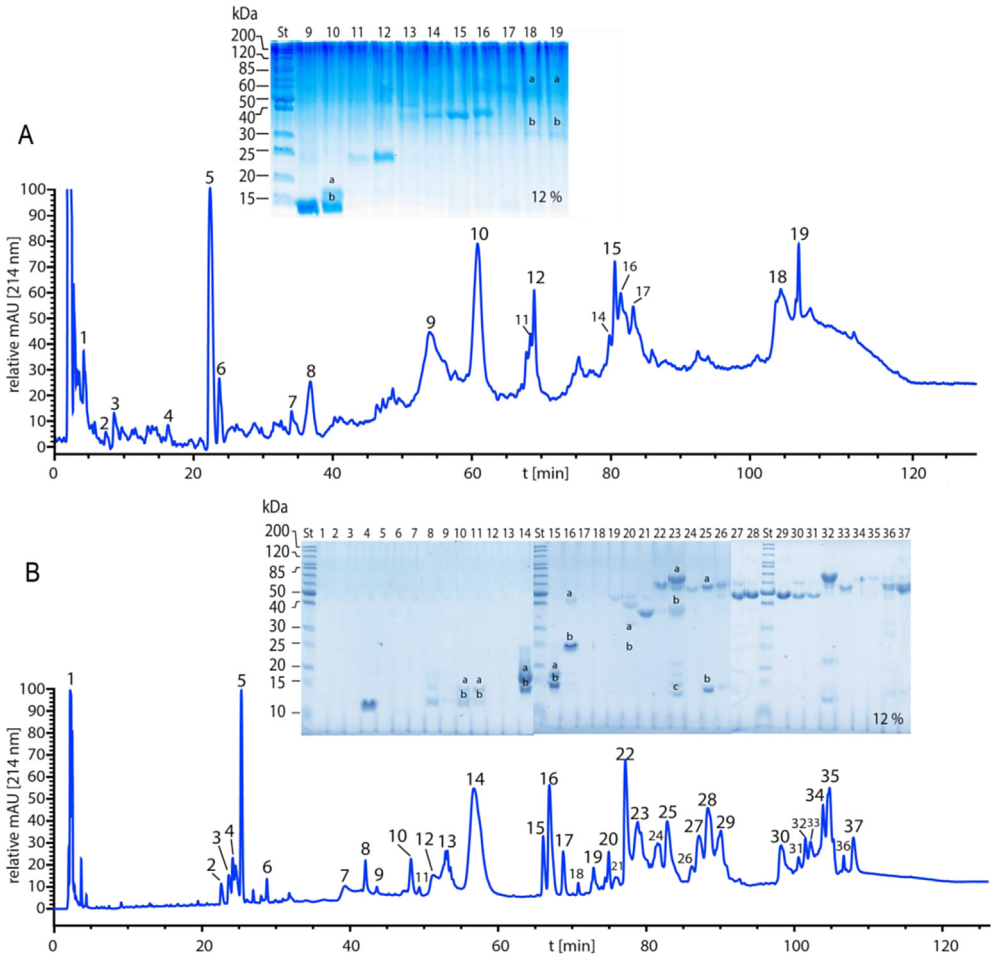

Fig. 3. Signal of the reverse-phase high-performance chromatographic separation. The UV_{214nm} signal for both chromatograms was set to relative percentage for each highest peak (Peak 5) with exception of injection peaks. **A** The *M. raddei* venom separation on UV_{214nm} signal. **B** The *M. bulgardahica* venom separation on UV_{214nm} signal. Fractions were analyzed by SDS-PAGE under reducing conditions.

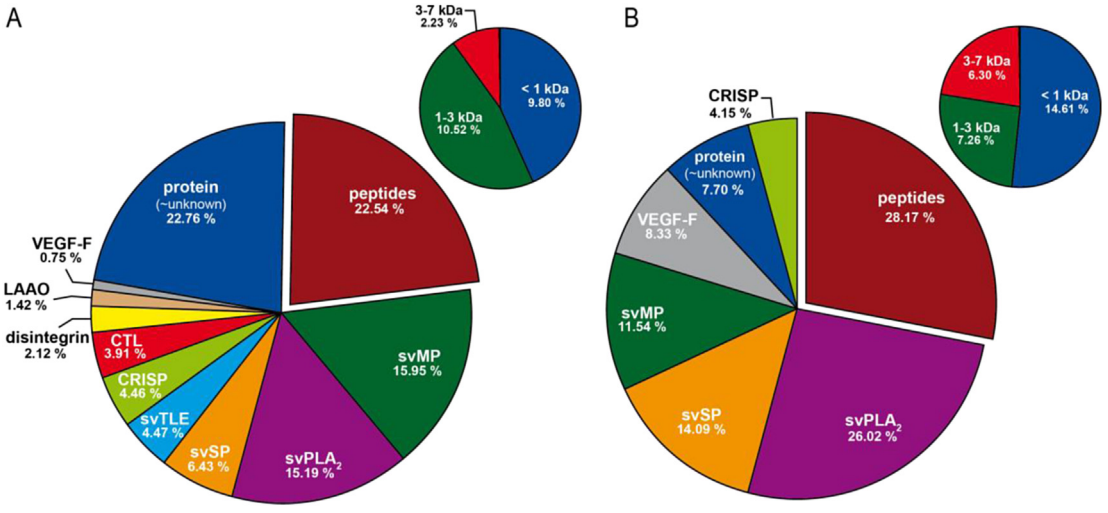

Fig. 4. Semi-quantitative venom composition of *M. bulgardahica* (A) and *M. raddei* (B). The pie chart represents the relative occurrence of different toxin families. In our analysis we identified snake venom metalloproteases (svMP); Phospholipases A_2 (PLA_2); snake venom serine proteases (svSP) and associated thrombin-like enzymes (svTLE); C-type lectins (CTL); disintegrins; L-amino acid oxidase (LAAO) and vascular endothelial growth factors (VEGF-F).

Based on the calculated IC_{50} values, the *M. bulgardaghica* venom has the most potent activity on A549 human lung carcinoma cells with an IC_{50} value of 2.60 ± 0.18 μg/mL while the *M. raddei* venom was exhibited the highest effect on CaCo-2 human colorectal carcinoma

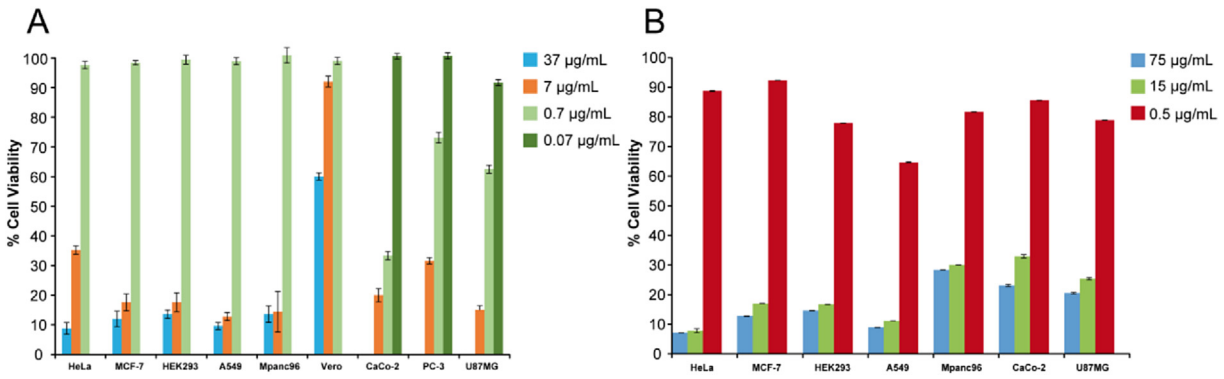

Fig. 5. Viability of cancer and non-cancerous cell lines after crude venom treatment for 48 h. Cell viability was determined by MTT assay, control was exposed to vehicle only which was taken as 100% viability. HeLa, human cervical epithelial carcinoma cells; MCF-7, human breast denocarcinoma epithelial cells; HEK293, human embryonic epithelial kidney cell; A549, human lung epithelial cells; MPanc-96, human pancreatic fibroblast cells; CaCo-2, human colon carcinoma epithelial cells; U87MG, human glioblastoma-astrocytoma epithelial-like cells; PC3, human prostate cancer cell line; VERO, African green monkey kidney cell. **A** Viability of cancer and non-cancerous cell lines after treatment with crude venom of *V. raddei.* **B** Viability of cancer and non-cancerous cell lines after treatment with crude venom of *V. bulgardahica.*

Table 3
IC_{50} values of *V. bulgardaghica and V. raddei* crude venom treated cell lines (positive control: Parthenolide). HeLa, human cervical epithelial carcinoma cells; MCF-7, human breast denocarcinoma epithelial cells; HEK293, human embryonic epithelial kidney cell; A549, human lung epithelial cells; MPanc-96, human pancreatic fibroblast cells; CaCo-2, human colon carcinoma epithelial cells; U87MG, human glioblastoma-astrocytoma epithelial-like cells; PC3, human prostate cancer cell line; VERO, African green monkey kidney cell.

Cell lines	*V. bulgardaghica* venom [µg/mL]	*V. raddei* venom [µg/mL]	Parthenolide [µg/mL]
CaCo-2	9.07 ± 0.25	0.65 ± 0.15	0.69 ± 0.18
MCF-7	6.14 ± 0.32	6.2 ± 1.19	1.17 ± 0.16
U87MG	6.04 ± 0.47	1.25 ± 0.38	1.93 ± 0.15
HeLa	4.34 ± 0.19	7.38 ± 1.52	3.33 ± 0.12
MPanc-96	8.38 ± 0.27	5.7 ± 1.02	0.58 ± 0.20
A549	2.60 ± 0.18	5.8 ± 1.78	1.66 ± 0.19
HEK293	4.42 ± 0.23	6.5 ± 0.87	0.63 ± 0.14
PC3	–	2,78 ± 0.27	1.8 ± 0.12
VERO	–	46.84 ± 2.42	2.58 ± 0.32

cell line with an IC_{50} = 0.65 ± 0.15 µg/mL, followed by U87MG (IC_{50} = 1.25 ± 0.38 µg/mL). In contrast to the effect of the *M. raddei* venom, CaCo-2 cells were found to be the highest resistant cell line to *M. bulgardaghica* venom (IC_{50} = 9.07 ± 0.25 µg/mL) while Vero (IC_{50} = 46.84 ± 2.42 µg/mL) and HeLa (IC_{50} = 7.38 ± 1.52 µg/mL) were more resistant compared to other cell lines. However, IC_{50} values of *M. xanthina* venom showed cytotoxicity against HT-29, Saos-2, MCF-7 and LNCap cells with IC_{50} values varying between 1.9 and 7.2 µg/mL, while a significant cytotoxicity was not observed against Hep3B and Vero cells at the maximum tested venom concentration (20 µg/mL) (Yalcin et al., 2014).

Previous studies, together with the results of the present report indicate that the *in vitro* cytotoxic activity of snake venoms is selective and depends on the cell line and snake species (Bradshaw et al., 2016; İğci et al., 2016; Jamunaa et al., 2012; Ozen et al., 2015; Yalcin et al., 2014). Bradshow et al. (Bradshaw et al., 2016) screened venoms from 61 taxa of venomous species on MCF-7 and A-375 cells and observed that Viperid venoms were more potent than Elapids and Colubrids. This selectivity can be linked to the venom variation, yielding different molecular mode of actions and receptor interactions which makes snake venom an attractive source of bioactive molecules for targeted cancer therapy (Bradshaw et al., 2016; Calderon et al., 2014; Ozen et al., 2015). Limited information is released regarding the anti-cancer and cytotoxic activity of *Montivipera* sp. venom in the literature, as discussed above. Thus, our results show that the venom of the viper species belonging to the genus *Montivipera* has great potential as a source of novel cytotoxic proteins. Since this is the first study in the literature regarding the venom of *M. bulgardaghica*, we further screened the reversed phase fractions in order to obtain more detailed information about its venom. *M. bulgardaghica* venom was most potent on the A549 cell line, an *in vitro* model cell line for non-small cell lung cancer. Therefore, this cell line was selected for the further screening. Among the tested fractions, *Montivipera bulgardaghica* fraction 21 (MBF21) was observed as the only potent fraction. MBF21 showed cytotoxic effects against A549 cells in a concentration-dependent manner with an IC_{50} value of 3.14 ± 0.11 µg/mL (see Fig. 6A). The effect of the MBF21 on the morphology of A549 cells was evaluated by inverted microscopy (see Fig. 6B). Morphological changes supported our cytotoxicity assay results for MBF21. Increased MBF21 concentration resulted in the damaged, rounding up and detachment of cells and multicellular aggregate formation. In addition, disorganization of the cells and large areas without cells were observed in the wells. Untreated cells were homogeneously adhered in wells, showing a normal phenotype. Interestingly, our results showed that this fraction contains a serine protease, but there is limited information regarding the *in vitro* or *in vivo* anti-cancer effects of SVSPs (Calderon et al., 2014). Generally, serine and metalloproteases are involved in the degradation of extracellular matrix proteins and facilitate tumor growth, invasion, metastasis and angiogenesis (Lopez-Otin and Matrisian, 2007). The elevated level of cellular proteases is used as prognostic biomarker and their inhibitors are considered to be potential anti-cancer drug candidates, in particular of molecules targeting matrix metalloproteases and plasminogen activators (Borgono and Diamandis, 2004; Lopez-Otin and Matrisian, 2007). In contrast, studies showed that extracellular proteases could also exhibit anti-cancer properties, including lung

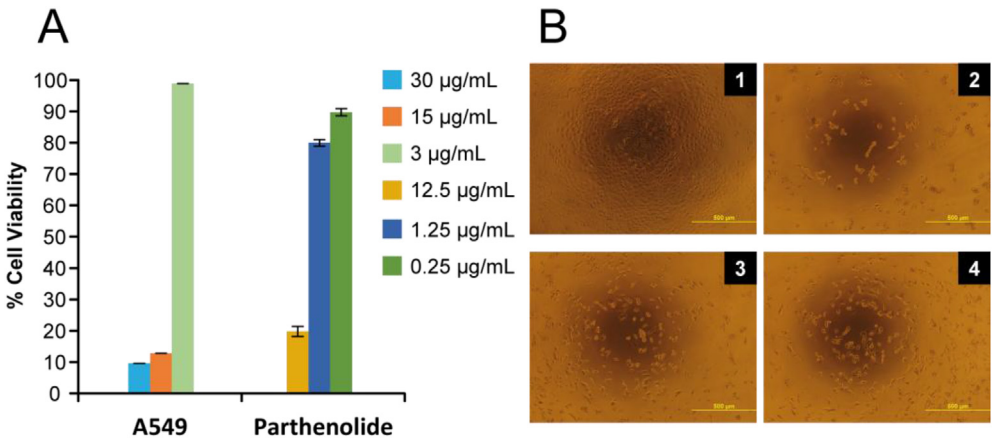

Fig. 6. **A** Viability of A549 cells after treatment with *V. bulgardaghica* venom fraction 21 (serine protease) for 48 h. Cell viability was determined in an MTT assay, normalized to a control (100% viability). **B** Effect of the isolated serine protease on A549 cells. Cells were treated with isolated serine protease from *V. bulgardaghica* (fraction 21) for 48 h at 37 °C. 1: untreated, 2: treated with fraction 21 (30 µg/mL), 3: treated with fraction 21 (15 µg/mL), 4: treated with fraction 21 (3 µg/mL).

cancer. Especially the human serine protease kallikreins (hKs) raised attention for their potential tumor-suppressive actions. It might activate transforming growth factor β (TGFβ), a central component of anti-mitotic pathways. Furthermore, serine proteases might inhibit cell migration through protease activated receptor (PAR) and have anti-angiogenic activity (Borgono and Diamandis, 2004; Lopez-Otin and Matrisian, 2007). The PAR activation mechanism is an important process also for the proliferation of alveolar capillary endothelial cells in primary lung adenocarcinomas (Jin et al., 2003). Furthermore, Sher et al. (2006) showed that overexpression of hK8 decreased the invasiveness of non-small cell lung cancer cells and suppressed tumor growth and cancer cell invasion *in vivo*.

Snake venom serine proteases are mainly found in viperid venoms and effect several steps of blood coagulation. Some of the SVSPs have a kallikrein-like (kinin-releasing) activity (Komori and Nikai, 2009). There are a few published papers about the anticancer effect of SVSPs. Markland (Markland, Jr, 1986) reported that crotalase, a serine protease from *Crotalus adamanteus*, inhibits the growth of B16 melanoma cells *in vitro* but this enzyme did not show promising activity *in vivo*. The effect of batroxobin, a thrombin-like serine protease from *Bothrops moojeni* venom was evaluated on artificial lung metastasis in mice in another study (Shibuya et al., 1990). Their results showed that batroxobin inhibited lung metastasis due to its defibrinogenating property and they found that its effect depends on natural killer cell activity of the host.

3.3. Conclusion

We reported the first proteomic characterization of the venom of *Montivipera bulgardaghica* by using the bottom-up approach combined with an initial intact mass profiling of the venom, which enabled us to detect ~98 venom components. The reduction of venom via TCEP indicated the existence of monomeric phospholipases A_2 with 7 intramolecular disulfide bridges and in addition we were able to identify a further phospholipase A_2 by a MS/MS experiment. By means of the intact mass profiling we could also identify two monomeric phospholipases A_2 with 7 intramolecular disulfide bridges for the *Montivipera raddei* venom. The initial mass profiling significantly improves the characterization of the complexity of snake venoms, but remains a challenging task for high molecular mass venom compounds, e.g. snake venom metalloproteases. With respect to the quantification of protein components it has to be mentioned that the UV peak area is only semi-quantitative and absolute quantities should be calculated with a new application based on isotopic labeled standards (Calderon-Celis et al., 2016). To further facilitate the proteomic analysis, the venom gland transcriptomic is a helpful technique and especially in combination with top-down venomics this gives you a more complete picture of venom diversity, so that transcriptomic analysis of both *Montivipera* species is indispensable and will be performed in the future (Calvete et al., 2017; Petras et al., 2016; Xu et al., 2017).

We further expand our analysis and described a detailed study of *in vitro* cytotoxicity against various cancer cell lines for the *Montivipera* species. The screening of components of *M. bulgardaghica* revealed a high inhibitory effect for a serine protease (IC_{50} 3.14 ± 0.11 µg/mL) against human alveolar adenocarcinoma (A-549) cells, which is one of the most common cancers with the highest mortality rate worldwide. Nevertheless, there is a need for the development of drug delivery systems or intra-tumor injection to increase the clinical application potential of cancer treatment for venom proteins and peptides due to their cytotoxic effect on normal cells. Furthermore, we showed the cytotoxic potential of *M. raddei* venom on various cancer cells. Elucidation of the tertiary structure and molecular mechanisms underlying cytotoxic effects could provide invaluable information and a great potential regarding the anti-cancer activities of SVSPs on lung cancer.

Acknowledgement

This study was supported by the Deutsche Forschungsgemeinschaft (DFG), Cluster of Excellence Unifying Concepts in Catalysis (UniCat) and by the Scientific and Technical Research Council of Turkey (TÜBİTAK) under Grant 111T338.

Appendix A. Supplementary data

Supplementary data related to this article can be found at http://dx.doi.org/10.1016/j.toxicon.2017.06.008.

References

Altschul, S.F., Gish, W., Miller, W., Myers, E.W., Lipman, D.J., 1990. Basic local alignment search tool. J. Mol. Biol. 215 (3), 403–410. http://dx.doi.org/10.1016/S0022-2836(05)80360-2.

Bazaa, A., Marrakchi, N., El Ayeb, M., Sanz, L., Calvete, J.J., 2005. Snake venomics: comparative analysis of the venom proteomes of the Tunisian snakes Cerastes

cerastes, Cerastes vipera and Macrovipera lebetina. Proteomics 5 (16), 4223–4235. http://dx.doi.org/10.1002/pmic.200402024.
Boettger, O., 1890. Eine neue Viper aus Armenien. Zool. Anz. 13, 62–64.
Borgono, C.A., Diamandis, E.P., 2004. The emerging roles of human tissue kallikreins in cancer. Nat. Rev. Cancer 4 (11), 876–890. http://dx.doi.org/10.1038/nrc1474.
Bradford, M.M., 1976. A rapid and sensitive method for the quantitation of microgram quantities of protein utilizing the principle of protein-dye binding. Anal. Biochem. 72 (1–2), 248–254. http://dx.doi.org/10.1016/0003-2697(76)90527-3.
Bradshaw, M.J., Saviola, A.J., Fesler, E., Mackessy, S.P., 2016. Evaluation of cytotoxic activities of snake venoms toward breast (MCF-7) and skin cancer (A-375) cell lines. Cytotechnology 68 (4), 687–700. http://dx.doi.org/10.1007/s10616-014-9820-2.
Calderon, L.A., Sobrinho, J.C., Zaqueo, K.D., Moura, A.A. de, Grabner, A.N., Mazzi, M.V., Marcussi, S., Nomizo, A., Fernandes, C.F.C., Zuliani, J.P., Carvalho, B.M.A., da Silva, S.L., Stabeli, R.G., Soares, A.M., 2014. Antitumoral activity of snake venom proteins: new trends in cancer therapy. Biomed. Res. Int. 2014 (203639) http://dx.doi.org/10.1155/2014/203639.
Calderon-Celis, F., Diez-Fernandez, S., Costa-Fernandez, J.M., Encinar, J.R., Calvete, J.J., Sanz-Medel, A., 2016. Elemental mass spectrometry for absolute intact protein quantification without protein-specific standards: application to snake venomics. Anal. Chem. 88 (19), 9699–9706. http://dx.doi.org/10.1021/acs.analchem.6b02585.
Calvete, J.J., 2011. Proteomic tools against the neglected pathology of snake bite envenoming. Expert Rev. Proteom. 8 (6), 739–758. http://dx.doi.org/10.1586/epr.11.61.
Calvete, J.J., 2014. Next-generation snake venomics: protein-locus resolution through venom proteome decomplexation. Expert Rev. Proteom. 11 (3), 315–329. http://dx.doi.org/10.1586/14789450.2014.900447.
Calvete, J.J., Juarez, P., Sanz, L., 2007. Snake venomics. Strategy and applications. J. Mass Spectrom. 42 (11), 1405–1414. http://dx.doi.org/10.1002/jms.1242.
Calvete, J.J., Petras, D., Calderón-Celis, F., Lomonte, B., Encinar, J.R., Sanz-Medel, A., 2017. Protein-species quantitative venomics: looking through a crystal ball. J. Venom. Anim. Toxins Incl. Trop. Dis. 23 http://dx.doi.org/10.1186/s40409-017-0116-9.
Chan, Y.S., Cheung, R.C.F., Xia, L., Wong, J.H., Ng, T.B., Chan, W.Y., 2016. Snake venom toxins: toxicity and medicinal applications. Appl. Microbiol. Biotechnol. 100 (14), 6165–6181. http://dx.doi.org/10.1007/s00253-016-7610-9.
Eichberg, S., Sanz, L., Calvete, J.J., Pla, D., 2015. Constructing comprehensive venom proteome reference maps for integrative venomics. Expert Rev. Proteom. 12 (5), 557–573. http://dx.doi.org/10.1586/14789450.2015.1073590.
Fox, J., Serrano, S., 2007. Approaching the golden age of natural product pharmaceuticals from venom libraries: an overview of toxins and toxin-derivatives currently involved in therapeutic or diagnostic applications. Curr. Pharm. Des. 13 (28), 2927–2934. http://dx.doi.org/10.2174/138161207782023739.
Fry, B.G., 2015. Venomous Reptiles and Their Toxins: Evolution, Pathophysiology and Biodiscovery. Oxford University Press, Oxford, UK.
Gerl, R., Vaux, D.L., 2005. Apoptosis in the development and treatment of cancer. Carcinogenesis 26 (2), 263–270. http://dx.doi.org/10.1093/carcin/bgh283.
Göçmen, B., Heiss, P., Petras, D., Nalbantsoy, A., Sussmuth, R.D., 2015. Mass spectrometry guided venom profiling and bioactivity screening of the Anatolian Meadow Viper, Vipera anatolica. Toxicon 107 (Pt B), 163–174. http://dx.doi.org/10.1016/j.toxicon.2015.09.013.
Harvey, A.L., 2014. Toxins and drug discovery. Toxicon 92, 193–200. http://dx.doi.org/10.1016/j.toxicon.2014.10.020.
IUCN, 2015. The IUCN Red List of Threatened Species.
İğci, N., Demiralp, D.O., 2012. A preliminary investigation into the venom proteome of Macrovipera lebetina obtusa (Dwigubsky, 1832) from Southeastern Anatolia by MALDI-TOF mass spectrometry and comparison of venom protein profiles with Macrovipera lebetina lebetina (Linnaeus, 1758) from Cyprus by 2D-PAGE. Arch. Toxicol. 86 (3), 441–451. http://dx.doi.org/10.1007/s00204-011-0763-5.
İğci, N., Nalbantsoy, A., Erkan, L.G., Akça, G.Y., Yalçın, H.T., Yalçın, M., Göçmen, B., 2016. Screening of cytotoxic, anti-angiogenic, anti-tumorogenic and antimicrobial activities of Anatolian Vipera ammodytes (Nose-horned viper) venom. Turk. J. Biochem. 41 (6) http://dx.doi.org/10.1515/tjb-2016-0195.
Jamunaa, A., Vejayan, J., Halijah, I., Sharifah, S.H., Ambu, S., 2012. Cytotoxicity of southeast asian snake venoms. J. Venom. Anim. Toxins Incl. Trop. Dis. 18 (2), 150–156. http://dx.doi.org/10.1590/S1678-91992012000200004.
Jin, E., Fujiwara, M., Pan, X., Ghazizadeh, M., Arai, S., Ohaki, Y., Kajiwara, K., Takemura, T., Kawanami, O., 2003. Protease-activated receptor (PAR)-1 and PAR-2 participate in the cell growth of alveolar capillary endothelium in primary lung adenocarcinomas. Cancer 97 (3), 703–713. http://dx.doi.org/10.1002/cncr.11087.
Juarez, P., Sanz, L., Calvete, J.J., 2004. Snake venomics: characterization of protein families in Sistrurus barbouri venom by cysteine mapping, N-terminal sequencing, and tandem mass spectrometry analysis. Proteomics 4 (2), 327–338. http://dx.doi.org/10.1002/pmic.200300628.
King, G.F. (Ed.), 2015. Venoms to Drugs: Venom as a Source for the Development of Human Therapeutics. Royal Society of Chemistry, London, UK.
Kini, R.M. (Ed.), 1997. Venom Phospholipase A2 Enzymes: Structure, Function and Mechanism. Wiley-VCH, Chichester, UK.
Komori, Y., Nikai, T., 2009. Chemistry and biochemistry of kallikrein-like enzym from snake venoms. J. Toxicol. Toxin. Rev. 17 (3), 261–277. http://dx.doi.org/10.3109/15569549809040394.
Laemmli, U.K., 1970. Cleavage of structural proteins during the assembly of the head of bacteriophage T4. Nature 227 (5259), 680–685.
Lewis, R.J., Garcia, M.L., 2003. Therapeutic potential of venom peptides. Nat. Rev. Drug Discov. 2 (10), 790–802. http://dx.doi.org/10.1038/nrd1197.
Lomonte, B., Calvete, J.J., 2017. Strategies in 'snake venomics' aiming at an integrative view of compositional, functional, and immunological characteristics of venoms. J. Venom. Anim. Toxins Incl. Trop. Dis. 23 (26) http://dx.doi.org/10.1186/s40409-017-0117-8.
Lopez-Otin, C., Matrisian, L.M., 2007. Emerging roles of proteases in tumour suppression. Nat. Rev. Cancer 7 (10), 800–808. http://dx.doi.org/10.1038/nrc2228.
Mackessy, S.P. (Ed.), 2010. Handbook of Venoms and Toxins of Reptiles. CRC Press, Boca Raton, USA.
Mallow, D., Ludwig, D., Nilson, G., 2003. True Vipers: Natural History and Toxinology of Old World Vipers. Krieger Publ, Malabar, USA.
Markland Jr., F.S., 1986. Antitumor action of crotalase, a defibrinogenating snake venom enzyme. Semin. Thromb. Hemost. 12 (4), 284–290. http://dx.doi.org/10.1055/s-2007-1003568.
Mosmann, T., 1983. Rapid colorimetric assay for cellular growth and survival: application to proliferation and cytotoxicity assays. J. Immunol. Methods 65 (1–2), 55–63.
Muth, T., Weilnbock, L., Rapp, E., Huber, C.G., Martens, L., Vaudel, M., Barsnes, H., 2014. DeNovoGUI: an open source graphical user interface for de novo sequencing of tandem mass spectra. J. Proteome Res. 13 (2), 1143–1146. http://dx.doi.org/10.1021/pr4008078.
Nalbantsoy, A., Karabay-Yavasoglu, N.U., Sayim, F., Deliloglu-Gurhan, I., Gocmen, B., Arikan, H., Yildiz, M.Z., 2012. Determination of in vivo toxicity and in vitro cytotoxicity of venom from the Cypriot blunt-nosed viper Macrovipera lebetina lebetina and antivenom production. J. Venom. Anim. Toxins Incl. Trop. Dis. 18 (2), 208–216. http://dx.doi.org/10.1590/S1678-91992012000200011.
Nalbantsoy, A., Erel, S.B., Koksal, C., Gocmen, B., Yildiz, M.Z., Karabay Yavasoglu, N.U., 2013. Viper venom induced inflammation with Montivipera xanthina (Gray, 1849) and the anti-snake venom activities of Artemisia absinthium L. in rat. Toxicon 65, 34–40. http://dx.doi.org/10.1016/j.toxicon.2012.12.017.
Nalbantsoy, A., İğci, N., Göçmen, B., Mebert, K., 2016. Cytotoxic potential of Wagner's viper, Montivipera wagneri, venom. North West J. Zool. 12 (2), 286–291.
Nilson, G., Andrén, C., 1986. The Mountain Vipers of the Middle East: the vipera Xanthina Complex (Reptilia, Viperidae). Zoolog. Forschungsinst. u. Museum Alexander Koenig, Bonn, DE.
Ozen, M.O., İğci, N., Yalçin, H.T., Göçmen, B., Nalbantsoy, A., 2015. Screening of cytotoxic and antimicrobial activity potential of Anatolian Macrovipera lebetina obtusa (Ophidia: Viperidae) crude venom. Front. Life Sci. 8 (4), 363–370. http://dx.doi.org/10.1080/21553769.2015.1055862.
Petras, D., Sanz, L., Segura, A., Herrera, M., Villalta, M., Solano, D., Vargas, M., Leon, G., Warrell, D.A., Theakston, R.D.G., Harrison, R.A., Durfa, N., Nasidi, A., Gutierrez, J.M., Calvete, J.J., 2011. Snake venomics of African spitting cobras: toxin composition and assessment of congeneric cross-reactivity of the pan-African EchiTAb-Plus-ICP antivenom by antivenomics and neutralization approaches. J. Proteome Res. 10 (3), 1266–1280. http://dx.doi.org/10.1021/pr101040f.
Petras, D., Heiss, P., Sussmuth, R.D., Calvete, J.J., 2015. Venom proteomics of indonesian king cobra, ophiophagus hannah: integrating top-down and bottom-up approaches. J. Proteome Res. 14 (6), 2539–2556. http://dx.doi.org/10.1021/acs.jproteome.5b00305.
Petras, D., Heiss, P., Harrison, R.A., Sussmuth, R.D., Calvete, J.J., 2016. Top-down venomics of the East African green mamba, Dendroaspis angusticeps, and the black mamba, Dendroaspis polylepis, highlight the complexity of their toxin arsenals. J. Proteom. 146, 148–164. http://dx.doi.org/10.1016/j.jprot.2016.06.018.
Sanz, L., Gibbs, H.L., Mackessy, S.P., Calvete, J.J., 2006. Venom proteomes of closely related Sistrurus rattlesnakes with divergent diets. J. Proteome Res. 5 (9), 2098–2112. http://dx.doi.org/10.1021/pr0602500.
Sanz, L., Ayvazyan, N., Calvete, J.J., 2008. Snake venomics of the Armenian mountain vipers Macrovipera lebetina obtusa and Vipera raddei. J. Proteome Res. 71 (2), 198–209. http://dx.doi.org/10.1016/j.jprot.2008.05.003.
Sawan, S., Yaacoub, T., Hraoui-Bloquet, S., Sadek, R., Hleihel, W., Fajloun, Z., Karam, M., 2017. Montivipera bornmuelleri venom selectively exhibits high cytotoxic effects on keratinocytes cancer cell lines. Exp. Toxicol. Pathol. http://dx.doi.org/10.1016/j.etp.2017.01.001.
Shanbhag, V.K.L., 2015. Applications of snake venoms in treatment of cancer. Asian Pac. J. Trop. Biomed. 5 (4), 275–276. http://dx.doi.org/10.1016/S2221-1691(15)30344-0.
Sher, Y.-P., Chou, C.-C., Chou, R.-H., Wu, H.-M., Wayne Chang, W.-S., Chen, C.-H., Yang, P.-C., Wu, C.-W., Yu, C.-L., Peck, K., 2006. Human kallikrein 8 protease confers a favorable clinical outcome in non-small cell lung cancer by suppressing tumor cell invasiveness. Cancer Res. 66 (24), 11763–11770. http://dx.doi.org/10.1158/0008-5472.CAN-06-3165.
Shibuya, M., Niitani, H., Aoyama, A., Kawachi, S., Nukariya, N., Baba, M., Iizuka, K., Sakai, S., Ohtsuka, M., 1990. Antimetastatic effect of defibrinogenation with batroxobin depends on the natural killer activity of host in mice. J. Cancer Res. Clin. Oncol. 116 (2), 168–172.
Six, D.A., Dennis, E.A., 2000. The expanding superfamily of phospholipase A2 enzymes: classification and characterization. Biochim. Biophys. Acta 1488 (1–2), 1–19. http://dx.doi.org/10.1016/S1388-1981(00)00105-0.
Stümpel, N., Rajabizadeh, M., Avci, A., Wuster, W., Joger, U., 2016. Phylogeny and diversification of mountain vipers (Montivipera, Nilson et al., 2001) triggered by multiple Plio-Pleistocene refugia and high-mountain topography in the Near and Middle East. Mol. Phylogenet. Evol. 101, 336–351. http://dx.doi.org/10.1016/j.ympev.2016.04.025.

Suzergoz, F., 2016. In vitro cytotoxic and proapoptotic activities of anatolian Macrovipera Lebetina Obtusa (Dwigubski, 1832) crude venom on cultured K562 Human Chronic Myelogenous Leukemia Cells. Int. J. Hematol. Oncol. 26 (1) http://dx.doi.org/10.4999/uhod.161104.

Vetter, I., Davis, J.L., Rash, L.D., Anangi, R., Mobli, M., Alewood, P.F., Lewis, R.J., King, G.F., 2011. Venomics: a new paradigm for natural products-based drug discovery. Amino acids 40 (1), 15–28. http://dx.doi.org/10.1007/s00726-010-0516-4.

Xu, N., Zhao, H.-Y., Yin, Y., Shen, S.-S., Shan, L.-L., Chen, C.-X., Zhang, Y.-X., Gao, J.-F., Ji, X., 2017. Combined venomics, antivenomics and venom gland transcriptome analysis of the monocoled cobra (Naja kaouthia) from China. J. Proteom. http://dx.doi.org/10.1016/j.jprot.2017.02.018.

Yalcin, H.T., Ozen, M.O., Gocmen, B., Nalbantsoy, A., 2014. Effect of ottoman viper (Montivipera xanthina (gray, 1849)) venom on various cancer cells and on microorganisms. Cytotechnology 66 (1), 87–94. http://dx.doi.org/10.1007/s10616-013-9540-z.